Environ. Sci. Technol. **2003**, *37,* 3367−3374

Molecular Interfacial Reactions between Pu(VI) and Manganese Oxide Minerals Manganite and Hausmannite

D. A. SHAUGHNESSY,[†] H. NITSCHE,*[,‡,§] C. H. BOOTH,[†] D. K. SHUH,[†] G. A. WAYCHUNAS,[||] R. E. WILSON,[†,§] H. GILL,[†,§] K. J. CANTRELL,[⊥] AND R. J. SERNE[⊥]

Chemical Sciences Division, Nuclear Science Division, and Earth Sciences Division, Lawrence Berkeley National Laboratory, Berkeley, California 94720, Department of Chemistry, University of California, Berkeley, California 94720, and Applied Geology and Geochemistry, Pacific Northwest National Laboratory, Richland, Washington 99352.

The sorption of Pu(VI) onto manganite (MnOOH) and hausmannite (Mn_3O_4) was studied as a function of time, solution pH, and initial plutonium concentration. Kinetic experiments indicate that the surface complexation of plutonium occurs over the first 24 h of contact with the mineral surface. The sorption increases with pH beginning at pH 3 until it reaches a maximum value of 100% at pH 8 (0.0011−0.84 μmol of Pu/m^2 of manganite and 0.98−1.2 μmol of Pu/m^2 of hausmannite) and then decreases over the pH range from 8 to 10. The ratio of solid to solution was 10 mg/mL for manganite experiments and 4 mg/mL for hausmannite samples. Carbonate was not excluded from the experiments. The amount of plutonium removed from the solution by the minerals is determined by a combination of factors including the plutonium solution species, the surface charge of the mineral, and the mineral surface area. X-ray absorption fine structure taken at the Pu L_{III} edge were compared to plutonium standard spectra and showed that Pu(VI) was reduced to Pu(IV) after contact with the minerals. Plutonium sorption to the mineral surface is consistent with an inner-sphere configuration, and no evidence of PuO_2 precipitation is observed. The reduction and complexation of Pu(VI) by manganese minerals has direct implications on possible migration of Pu(VI) species in the environment.

Introduction

Several U.S. Department of Energy sites have been contaminated with plutonium as a result of weapons-related activities. Plutonium is highly toxic and potentially mobile in aquatic environments such as the vadose zone. Risk assessment studies, which predict the potential hazards of plutonium and other transuranic nuclides in the environment, require reliable models of plutonium transport through the vadose zone to nearby groundwater supplies. Fundamental knowledge of the interfacial reactions between plutonium and the surrounding geomaterial is essential for modeling the potential transport of plutonium through the vadose zone as well as forming an accurate assessment of the risks this radionuclide poses to the surrounding population.

Previous studies have shown that Pu(IV) and Pu(V) will adsorb to iron oxyhydroxides, manganese oxide soil components, and other naturally occurring materials, possibly retarding its migration through the environment (*1*−*3*). Plutonium can coexist in four oxidation states (+3, +4, +5, and +6) under environmental conditions, with the oxidized forms (+5, +6) being largely soluble (*4*). It is highly redox active, which means that after contact with the surrounding environment the more soluble, oxidized forms of plutonium could potentially be reduced and therefore become more insoluble. Recent synchrotron-based X-ray microprobe studies have shown that in a mixed mineral system it was the manganese oxides and not the iron oxides that preferentially sequestered plutonium, even though the iron was present in larger quantities (*5*). On the basis of these initial findings, an effective transport model and remediation system for plutonium contaminants requires a thorough understanding of the interactions between plutonium and manganese oxyhydroxides.

There are a wide range of manganese oxyhydroxide minerals found in the environment resulting from the oxidation of soluble, aqueous Mn(II) by both abiotic and biotic means (*6*, *7*). They are most commonly found as coatings on soil and sediment grains. These minerals exist in a wide variety of structures including those with tunnels, layers, and other configurations (*8*) with manganese in several different oxidation states and structural motifs offering a variety of reactive sites for the sorption or incorporation of trace metal species. Manganese oxides can have high negative surface charges over a wide pH range (pH ≥2), resulting in a large cation sorption capacity (*9*).

We have begun systematic studies of the interfacial reactions between aqueous plutonium species and manganese oxyhydroxide mineral surfaces starting with the interactions of Pu(VI) with manganite (MnOOH) and hausmannite (Mn_3O_4). These minerals were chosen as representative examples of manganese oxyhydroxides typically found in vadose zone conditions beneath the tank farms at the Hanford site (*10*, *11*). Figure 1 illustrates the (a) manganite and (b) hausmannite structures. Manganite has a structure realted to rutile (*12*) and is composed of rows of edge-sharing Mn-$(O,OH)_6$ octahedra (*8*), which are considerably distorted. Hausmannite is a mixed valence manganese oxide having a tetragonally distorted spinel structure with most Mn(III) in octahedral sites and the Mn(II) in tetrahedral coordination (*8*). The information obtained from these studies can be incorporated into models for the prediction of migration of plutonium species in the environment.

Experimental Procedures

Minerals. Both manganite and hausmannite were supplied by Chemetals, Inc. (Baltimore, MD) as dry powders. The minerals were crushed and sieved and the 63−212- and ≤20-μm size fractions were collected. Powder X-ray diffraction (XRD) patterns were collected on a Siemens D-500 diffrac-

* Corresponding author phone: (510)486-5615; fax: (510)486-7444; e-mail: hnitsche@lbl.gov.

[†] Chemical Sciences Division, Lawrence Berkeley National Laboratory.

[‡] Nuclear Science Division, Lawrence Berkeley National Laboratory.

[§] University of California.

[||] Earth Sciences Division, Lawrence Berkeley National Laboratory.

[⊥] Pacific Northwest National Laboratory.

10.1021/es025989z CCC: $25.00
Published on Web 06/28/2003

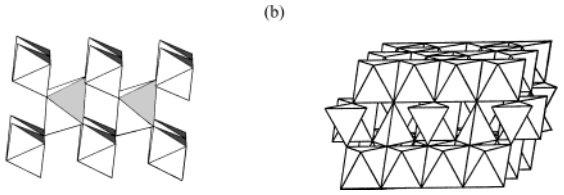

FIGURE 1. Structures of the manganese oxyhydroxide minerals (a) manganite and (b) hausmannite.

tometer with Cu Kα radiation. The XRD patterns confirmed the respective mineral phases and yielded no evidence of significant impurities or interfering phases within the detection limit of the method. The surface areas were determined on the 63−212-μm size fraction by nitrogen adsorption using the standard BET method with an outgassing temperature of 150 °C. The surface area of manganite is 9.5 ± 1.4 m^2/g, and hausmannite has a surface area of 20.4 ± 0.8 m^2/g.

The pH of the point of zero surface charge (pH_{PZC}) was determined for each mineral using potentiometric titration according to the method of Parks and de Bruyn (*13*). Suspensions of manganite (0.5 g of manganite/15 mL of $NaClO_4$) and hausmannite (1 g/15 mL of $NaClO_4$) were prepared at ionic strength values ranging from 0.005 to 0.1 M and were sparged with Ar to eliminate CO_2 species. Titrations were performed for each ionic strength at 25 °C with an Orion 960 Autochemistry System and consisted of a base titration using 0.05 M NaOH and an acid titration using 0.05 M $HClO_4$. During the titrations, the headspace was covered with Ar to exclude atmospheric CO_2 contamination, and the acids and bases were prepared in a CO_2-free glovebox that was continuously flushed with Ar. The surface charge densities as a function of pH were determined from the titration data. The intersection of surface charge data at different ionic strengths gives the pH_{PZC}. For manganite, this point occurs at a pH of 7.4 ± 0.3. The pH_{PZC} of hausmannite could not be exactly determined as it falls outside of the reliable working range of the pH electrode but was found to be greater than 10.

Sorption Experiments. All sorption experiments were performed with minerals from the 63−212-μm size fraction. Kinetic experiments were performed over the course of 30 d in polypropylene cones that were previously washed in 0.1 M $HClO_4$ and rinsed with double distilled water. No adsorption of plutonium onto the walls of the cones was found in the pH range from 3 to 10. Solutions of $^{239}Pu(VI)$ were prepared by first fuming the plutonium stock solution with concentrated nitric acid to destroy any organic material that may be present as a safety precaution for the following steps with perchloric acid. *Caution: The presence of any organic material, even the smallest amounts, may cause an explosion when it gets in contact with hot perchloric acid!* After three repetitions with the nitric acid, concentrated perchloric acid (70% double distilled from VYCOR, G. F. Smith) was added to the stock solution and refluxed at 190 °C for 4 h to oxidize the plutonium to Pu(VI). Manipulation of plutonium was performed inside of a negative pressure glovebox. All steps with nitric and perchloric acids were performed in specially designed glassware to prevent the accumulation of hot perchlorate and nitrate vapors inside the glovebox and to prevent the formation of explosive perchlorate. The oxidation state of the stock solution was verified using optical absorption spectroscopy performed on an Ocean Optics S2000 fiber optic spectrometer. Pu(VI) was identified based on its characteristic absorption spectrum (*14*), and no other oxidation states were present. An aliquot of the Pu(VI) stock solution was brought to the desired pH using $HClO_4$ or NaOH, and an appropriate amount of 1 M $NaClO_4$ was added to bring the ionic strength of the solution to 0.1 M. At pH values greater than 7, $NaHCO_3$ was added to achieve equilibrium with air (calculated ahead of time using carbonate equilibrium with $\log K_H = -1.47$, $\log K_1 = -6.16$, and $\log K_2 = -9.94$). The Pu solutions were equilibrated overnight at the desired pH, and the pH values were monitored before adding the minerals. pH drift of the solutions was negligible during this time frame; 250 mg of manganite or 100 mg of hausmannite was added to the Pu solutions, and the slurry was slowly rocked end over end for 30 d. The total sample volume was 25 mL, and the plutonium solution concentration ranged from 1×10^{-7} to 1×10^{-4} M. The ratio of solid to solution was 10 mg/mL for manganite and 4 mg/mL for the hausmannite experiments. The amount of plutonium sorbed onto the minerals was determined by calculating the difference between the initial concentration of plutonium in solution and the amount of plutonium remaining in solution after contact. At specific time intervals, a 250-μL aliquot was removed from the sample and the solid and supernatant were separated using a Microcon YM-30 cellulose centrifugal filter at 10 000 rpm for 12 min. The filters were used without any prior treatment, and plutonium adsorption on the filters was found to be negligible in the pH ranges used in these experiments. Two 100-μL aliquots of the resulting solution were each added to 5 mL of Ecolume scintillation cocktail and counted using a LKB Wallac, 1219 Rackbeta liquid scintillation counter with α/β discrimination to determine the concentration of plutonium remaining in solution.

Separate batch experiments were conducted to determine sorption as a function of pH using a fixed reaction time. Samples were prepared as described above, except that the total sample volume was 2.5 mL and either 25 mg of manganite or 10 mg of hausmannite was added to the Pu(VI) solution, which had been previously equilibrated at the desired pH. The ratios of solid to solution were the same as those used in the kinetic determinations. Ionic strength values were fixed at 0.1 M. After 24 h of rocking, 50 μL of the samples was removed, and two 25-μL aliquots were each added to 3 mL of Ecolume scintillation cocktail for measurement via liquid scintillation counting.

Blank solutions of Pu(VI) at 1×10^{-4} M in 0.1 M $NaClO_4$ were prepared in the same polypropylene cones used in the sorption experiments at several pH values ranging from 3 to 8. These solutions were monitored over the 30-d time period of the experiments using optical absorption spectroscopy. The plutonium in these blank solutions remained as Pu(VI) over the entire 30-d monitoring period.

X-ray Absorption Fine Structure (XAFS). Samples for XAFS measurements were prepared as described above for the kinetic studies except that minerals from the ≤20-μm size fraction were used in order to reduce the possibility of thickness effects. Separate experiments showed that the sorption behavior of the ≤20-μm size fractions were identical to those of the 63−212-μm size fraction. After 24 h of contact time with the mineral, the solids were filtered onto 3-μm cellulose membrane filters (1 in. diameter), which were then sealed inside multiple polyethylene bags for containment. The solids on the filters were measured as wet pastes and not as dry solids.

Plutonium L_{III} edge XAFS spectra were collected at the Stanford Synchrotron Radiation Laboratory (SSRL) on wiggler beam line 4-1 using a half-tuned Si(220) double-crystal monochromator and a 0.7-mm vertical slit opening. Fluorescence yield spectra were collected with a four-pixel Ge fluorescence detector (*15*). Energy calibration was performed simultaneously by measuring transmission data from a PuO_2 reference. The Pu reference energy was set to 18,057 eV, taken from the peak in the first derivative. All data reduction and fits to the data utilize standard procedures (*16*, *17*), and data from the Ge detector was corrected for dead time prior to data reduction. Backscattering amplitudes and phases for fitting the raw data were calculated with FEFF8 (*18*).

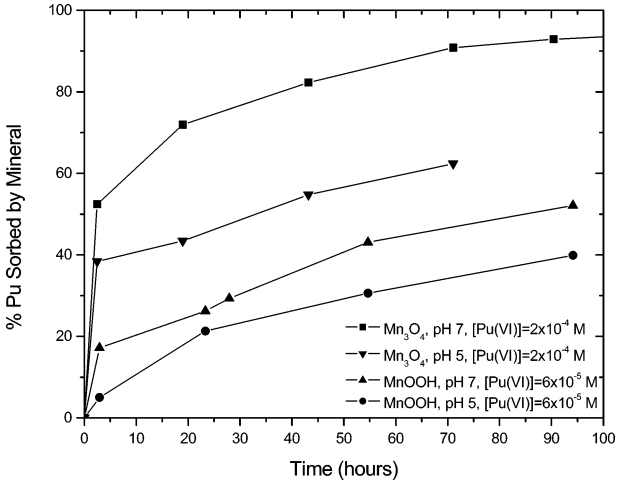

FIGURE 2. Sorption of plutonium onto manganite and hausmannite as a function of time. Plutonium concentrations are given as the initial concentration of Pu(VI) in solution prior to the addition of any minerals. Total sample volume was 25 mL in each experiment, and the ratio of solid to solution was 10 mg/mL for manganite and 4 mg/mL for hausmannite. Error bars are contained within the points.

Results and Discussion

Sorption Kinetics. Sorption of plutonium (initially present as Pu(VI)) onto manganite and hausmannite as a function of time was studied at several pH values with varying plutonium concentrations. The total sample volume was 25 mL for each experiment, and the ratio of solid to solution was 10 mg/mL for manganite and 4 mg/mL for hausmannite. Figure 2 shows several examples of these kinetic experiments. There appears to be an initial, rapid sorption step that occurs within the first 24 h of contact followed by a much slower sorption process that continues for a longer period of time. This behavior was observed in experiments with both manganite and hausmannite, regardless of pH, initial plutonium concentration, or mineral size fraction. Based on the results of these kinetic studies, subsequent sorption experiments were measured over a 24-h period in order to avoid any secondary reactions.

This two-step process has been observed previously in sorption studies of transition metal cations on mineral surfaces including iron and manganese oxyhydroxides (*19*−*22*). The actinides also appear to follow this kinetic behavior based on sorption experiments of uranium and neptunium onto iron oxyhydroxide surfaces (*23*−*25*) and the sorption of plutonium on various minerals including δ-MnO_2 (*3*, *26*). The rapid step has been attributed to a diffusion-controlled surface reaction while the slower step is most likely a combination of different processes, possibly including surface precipitation, micropore diffusion, structural rearrangement of surface species, and others (*27*). The exact mechanisms that determine the sorption rates of cations onto mineral surfaces are not yet entirely understood (*27*).

pH Dependence. The sorption of plutonium (originally Pu(VI)) on manganite and hausmannite as a function of pH and plutonium concentration is shown in Figure 3. Total sample volume was 2.5 mL for each experiment, and the solid to solution ratios were the same as those used in the kinetic experiments previously discussed. The amount of plutonium sorbed onto manganite (Figure 3a) increased from 0% at pH 3 to a maximum value of 100% at pH 8 and decreased in the pH region between 9 and 10. At the sorption maxima, the ratios of total Pu sorbed to the total available surface area ranged from 0.0011 to 0.84 μmol of Pu/m^2. The shape of these sorption curves is indicative of cation sorption on hydrous oxides (*28*). The pH edge is shifted to slightly higher values when the ratio of aqueous plutonium ion concentration to number of surface sites is increased. This shift of the sorption edge is caused by a saturation of surface sites when the metal ion to surface site ratio is high and has been observed in the sorption of both transition metal cations and actinide cations onto various mineral surfaces including iron oxyhydroxides (*22*, *23*, *28*−*31*).

Figure 3b shows the sorption of plutonium onto hausmannite at varying pH values. Once again, there appears to be a shift in the pH edge to higher values when a larger starting plutonium concentration is used, and the amount of sorption decreases at pH values between 9 and 10. At the pH values corresponding to maximum sorption, the ratios of total sorbed plutonium to total available surface area ranged from 0.98 to 1.2 μmol of Pu/m^2.

The sorption of plutonium on these minerals is due to the interaction between the plutonium solution species and the surface functional groups of the minerals, which have been shown to be hydroxyl groups for manganese oxides as well

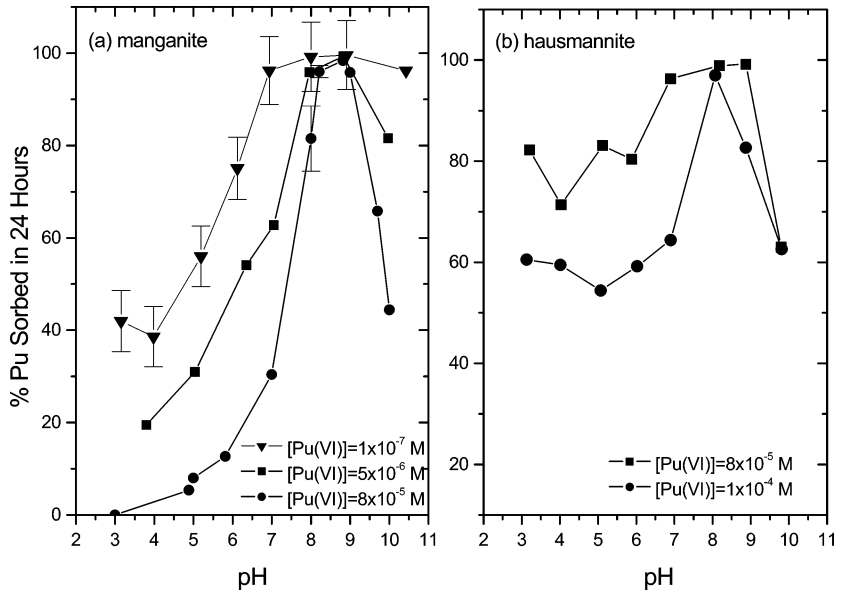

FIGURE 3. Sorption of plutonium onto (a) manganite and (b) hausmannite as a function of pH and initial Pu(VI) concentration prior to the addition of minerals after a 24-h contact time. Total sample volume was 2.5 mL in each experiment. Solid to solution ratios were the same as those in Figure 2. Error bars not shown are contained within the points.

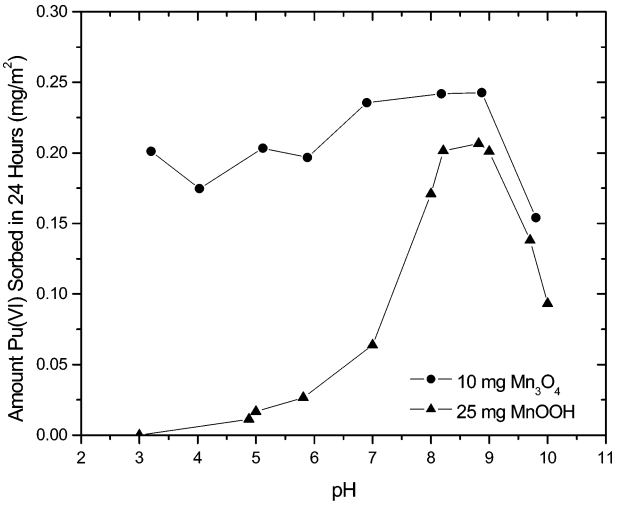

FIGURE 4. Sorption of plutonium initially present as Pu(VI) at a concentration of 8 × 10^{-5} M onto manganite and hausmannite per unit surface area. The contact time between the Pu and the minerals was 24 h. Sample volumes and solid loadings were the same as those in Figure 3.

as a variety of other oxide minerals (*32*, *33*). Cations can sorb onto mineral oxide surfaces in response to both chemical and electrostatic phenomena (*27*). The strong dependence on pH illustrated in Figure 3 is primarily the result of the net charge on these mineral surfaces. At low pH values the surface hydroxyl groups are protonated, resulting in a net positive surface charge whereas at higher pH the surface has a net negative charge due to deprotonated surface hydroxyl groups (or adsorption of hydroxide anions.) As the pH increases, the overall positive charge of the surface decreases, making the electrostatic attraction between the mineral surface and the cationic solution species more dominant (*33*). Previous investigations of cation sorption onto oxide surfaces have shown that the sorption process is usually accompanied by the release of protons (or adsorption of hydroxide anions) by the surface (*34*, *35*). The extent of plutonium sorption would therefore depend on the protonation stoichiometry of the surface, the plutonium species in solution, and the sorbed plutonium−surface complexes. Unfortunately, the actual stoichiometry of cation sorption processes is not yet fully understood (*27*). It has also been previously observed that metal cations can strongly sorb to mineral surfaces even against electrostatic repulsion (*34*, *35*). This implies that the complexation chemistry of metal cations with surface hydroxyl groups can be even more dominant than electrostatic forces in driving metal cation sorption (*27*). The decreased sorption in the weakly alkaline regions in Figure 3 is due to repulsion between the surface, which has an increased negative surface charge, and anionic plutonium hydroxide or carbonate complexes in solution, which form at these higher pH values. Similar results have been observed with actinide sorption onto mineral surfaces in the presence of CO_2 (*2*, *23*, *36*−*38*).

In comparing Figure 3, panels a and b, it appears that more plutonium is sorbed to the hausmannite surface than to manganite under the same conditions. This can be attributed to a larger surface site density on hausmannite. Figure 4 illustrates this point by showing the sorption of plutonium (initially Pu(VI)) at a starting concentration of 8 × 10^{-5} M onto manganite and hausmannite per unit surface area of the mineral. This figure implies that there are more active hausmannite surface sites available for plutonium to bind to than on the manganite surface. This assumes that the protonation stoichiometries of both mineral surfaces are relatively similar, which may not be correct. If the surface protonations varied greatly, this could also explain the difference in plutonium sorption on hausmannite as compared to manganite under the same experimental conditions.

Plutonium Valence Determination. The oxidation states of the plutonium sorbed to the mineral surfaces and the plutonium remaining in solution after sorption was complete were determined using XAFS and optical absorption methods. To determine the oxidation state of the plutonium bound to the surfaces, X-ray absorption near-edge structure (XANES) measurements were made. Plutonium oxidation states can be determined by carefully comparing the main L_{III} absorption edge energy to those of known standards (*39*−*42*). In addition to the actual sorption samples, XANES spectra were also collected from standard solutions containing either Pu(IV), Pu(V), or Pu(VI) (the oxidation states of the plutonium standards were verified prior to and during measurement using optical absorption spectroscopy.) Pu(VI) was prepared using the method described previously and was measured as a 1 × 10^{-3} M solution in concentrated $HClO_4$. Pu(V) (1 × 10^{-4} M, pH 3) and Pu(IV) (1 × 10^{-3} M, pH 0) were prepared by electrochemically reducing a solution of Pu(VI) in $HClO_4$ according to the method of Cohen (*43*). The incident X-ray energies for the Pu L_{III} edges of the standard solutions were calibrated to the PuO_2 reference. There are energy differences between the Pu(IV), Pu(V), and Pu(VI) standards and the PuO_2 reference (1.88 ± 0.03, 0.17 ± 0.03, and 2.33 ± 0.03 eV, respectively, taken from the peak in the first derivative where the errors are the deviation of the mean of all individual traces). Furthermore, there is a feature on the high energy side of the white line in the Pu(V) and Pu(VI) spectra due to multiple scattering between the plutonium and the axial oxygens of the plutonyl structure. Because of the change in coordination going from Pu(IV) to the plutonyl structure, there is not a linear energy shift from Pu(IV) to Pu(V); this anomalous energy shift has been observed previously (*39*, *40*). These differences in energy and shape allow for the determination of plutonium oxidation states on the mineral surfaces by fitting a linear combination of the standard spectra to the experimental data between 18 000 and 18 080 eV. This method has been verified using chemical extraction methods (*41*). In addition, optical absorption spectroscopy was used to determine the valence of the plutonium remaining in solution after the sorption process was completed. The minerals were filtered out, and the resulting supernatant was measured from 400 to 900 nm. Thus, the combination of XANES and optical absorption measurements allow us to reliably determine the valence of both the sorbed plutonium and the plutonium remaining in solution.

XANES measurements collected from plutonium sorbed onto the minerals are shown in Figure 5a, and Figure 5b shows the XANES collected from the standard solutions. A comparison of the plutonium standards to the mineral data shows that the plutonium sorbed to manganite or hausmannite has been reduced from the initial Pu(VI) state to the Pu(IV) oxidation state. Table 1 gives the distribution of plutonium oxidation states on the mineral surface in each sample, and Figure 6 shows an example of the fits applied to the XANES data. In all of the XANES spectra presented in Figure 5a, the distinctive plutonyl feature is missing, indicating that the original plutonyl cations are sorbed to these surfaces as Pu(IV). Figure 7 shows the optical absorption spectrum of an original Pu(VI) solution at pH 5 before manganite was added and the subsequent spectra taken of the solution at specific time intervals after the mineral had been added. After 24 h of contact with manganite, the plutonium remaining in solution after sorption has been reduced to Pu(V). Without any manganite present, a blank solution of Pu(VI) prepared under the same conditions remained as Pu(VI) during this same time frame; therefore,

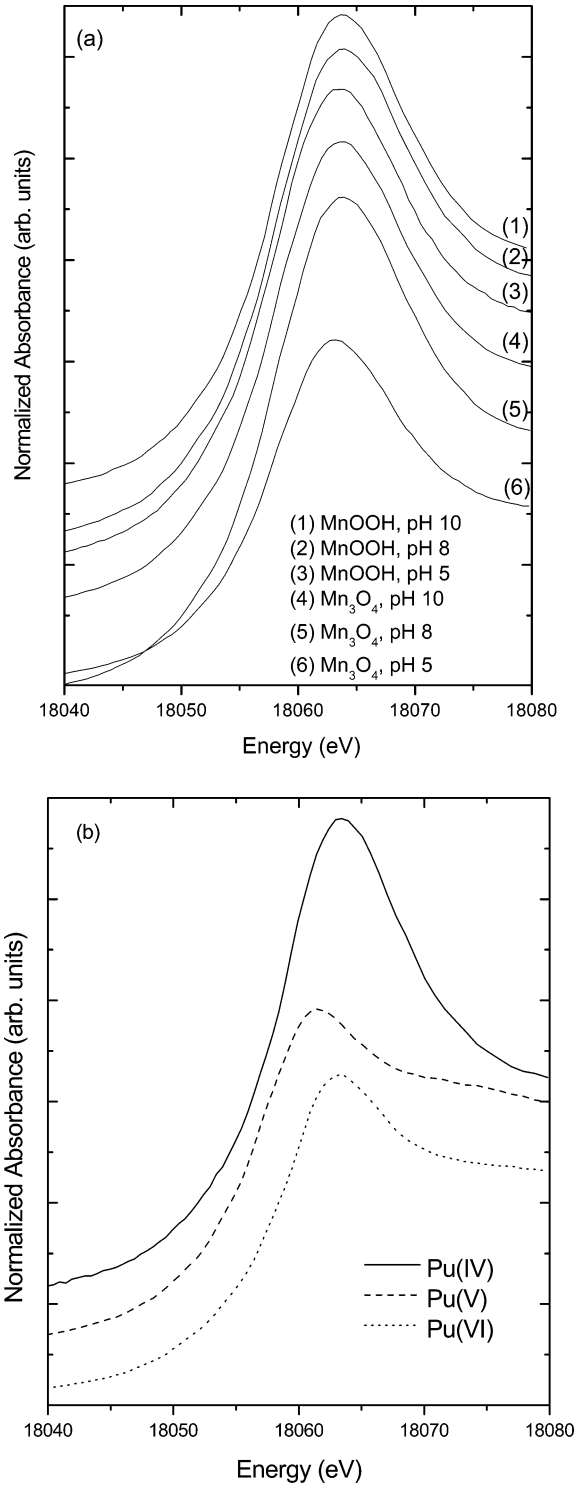

FIGURE 5. XANES spectra of (a) plutonium initially present as 1×10^{-4} M Pu(VI) sorbed onto manganite and hausmannite after 24 h of contact at several pH values and (b) Pu(IV), Pu(V), and Pu(VI) standard solutions. The shoulder around 18070 eV in the Pu(V) and Pu(VI) spectra is due to multiple scattering between the plutonium and the axial oxygens. Sample volumes and solid to solution ratios were the same as those in Figure 2.

contact with the mineral was responsible for the reduction of plutonium. The same results were observed with hausmannite. No Pu(IV) was observed in these optical absorption spectra. The combination of the XANES spectra and the optical absorption data shows that all of the initial Pu(VI) has been reduced to either Pu(V) in solution or Pu(IV) on the mineral surfaces. This implies that Pu(IV) has a stronger

TABLE 1. Distribution of Plutonium Oxidation States on Mineral Surface from Sorption of a Pu(VI) Solution[a]

mineral added	pH	Pu(IV) (%)	Pu(V) (%)	Pu(VI) (%)
MnOOH	5	68	32	0
MnOOH	8	55	35	10
MnOOH	10	66	32	2
Mn_3O_4	5	71	29	0
Mn_3O_4	8	58	36	6
Mn_3O_4	10	62	38	0

[a] Determined by fitting the XANES data in Figure 5a with a linear combination of the plutonium standards shown in Figure 5b. The contact time between the plutonium and the minerals was 24 h. Errors in the XANES fits were calculated from the diagonal terms of the covariance matrix assuming that χ^2 divided by the number of degrees of freedom was equal to unity and were equal to ±5% for each value. The plutonium remaining in solution after the sorption was finished was all in the Pu(V) oxidation state.

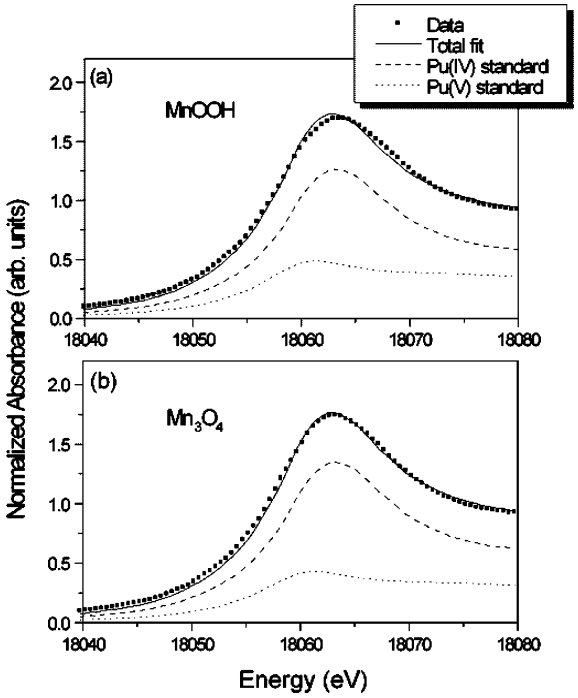

FIGURE 6. XANES spectra of (a) manganite and (b) hausmannite after a 24-h contact time with 1×10^{-4} M Pu(VI) solutions at pH 5. The spectra were fit with a linear combination of the plutonium standard spectra. The overall fits as well as the plutonium standards used to fit the data are shown in their relative amounts.

interaction with the surface functional groups than Pu(V). Once the Pu(IV) is formed, it is immediately bound to the mineral surface and removed from solution whereas the Pu(V) is found in the solution phase. Since the XANES samples were measured as wet pastes, based on the optical absorbance spectra, it is likely that the Pu(V) observed in the fits to the XANES data (Figure 6) is present only in the solution phase of these samples and not from sorption of Pu(V) on the mineral surfaces.

One plausible explanation for the observed redox between Pu(VI) and these manganese oxyhydroxide minerals is the presence of Mn(II) phases. Mn(II) is highly soluble, and its presence in solution could account for the rapid reduction of plutonium to the Pu(IV) state, which would then sorb to the minerals. XAFS studies have shown that the surfaces of these minerals change after exposure to the atmosphere (*44*). Surface alteration layers containing Mn(II) could form on these minerals prior to contact with plutonium. Solubilized Mn(II) from these layers would then be responsible for the

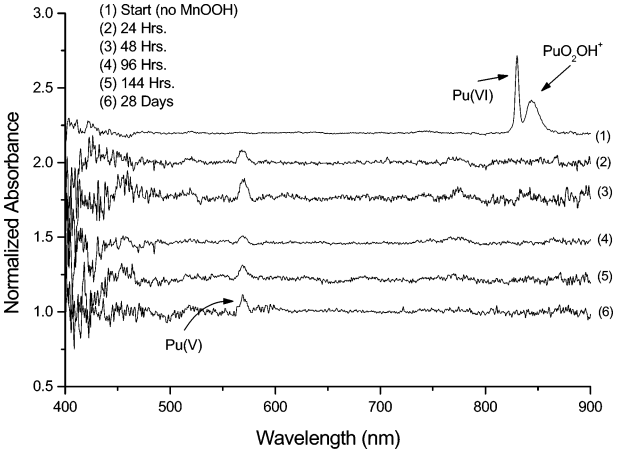

FIGURE 7. Optical absorbance spectra taken of the solution (the minerals were filtered out) from the interaction of a 1×10^{-4} M Pu(VI) solution with manganite at pH 5. See Figure 2 for sample volume and solid loading. After 24 h of contact, the Pu(VI) and its first hydrolysis product are reduced to Pu(V) in solution. A Pu(VI) solution prepared in the same manner without any manganite present is stable as Pu(VI) over this time period. The same results were observed when Pu(VI) was placed in contact with hausmannite.

observed plutonium redox. Other possible surface alteration layers, such as carbonate species, might also contribute to the reduction of plutonium. Mn(II) can also be formed via disproportionation of Mn(III) to Mn(IV) and Mn(II). Even though no Mn(II) phases were observed in the XRD spectra, the technique is not sensitive enough to see minor impurities or amorphous phases containing Mn(II) that may be present on the surface layers of these minerals. Further study of the mineral surface is necessary in order to identify the reductant-(s) responsible for the observed redox interactions between oxidized plutonium and these manganese oxyhydroxides.

The spectra suggest that the plutonium is first reduced from Pu(VI) to Pu(V) in solution. It is not clear whether the Pu(V) is further reduced in solution to Pu(IV), which then binds to the mineral surface, or if Pu(V) is reduced to Pu(IV) after sorbing to the minerals. The Pu(IV) on the mineral surfaces is not due solely to disproportionation of Pu(V). If all of the Pu(VI) was first reduced completely to Pu(V), the Pu(V) could undergo disproportionation under acidic conditions according to the following reaction (*4*):

$$2PuO_2^{+} + 4H^{+} \leftrightarrow Pu^{4+} + PuO_2^{2+} + 2H_2O \qquad (1)$$

If this occurred first in solution, the Pu(IV) would then sorb to the minerals. However, the amount of Pu(IV) observed on the mineral surfaces is more than what could be formed via disproportionation of Pu(V) after 24 h based on the most recently published disproportionation rates (*45*), unless it was somehow catalyzed at the mineral surface. Likewise, the formation of Pu(IV) is not due to auto-reduction of Pu(VI) based on the rate of auto-reduction reported in ref *46*. While these two processes do contribute to the overall amount of Pu(IV) observed in these systems, it appears that contact with the minerals is the primary driving force behind the reduction of plutonium to the Pu(IV) state.

Regardless of the pathway by which the plutonium is reduced to Pu(IV), the redox reactions between the plutonium and these manganese oxyhydroxides must be considered when discussing the sorption of plutonium as a function of pH as described in the previous section. If the protonation stoichiometry of both the plutonium species and surface functional groups is the driving force behind these sorption reactions, then redox interactions must play an important role as well. More study into these systems is required to fully understand the overall sorption reaction, which is most likely a combination of redox reactions, electrostatic forces, and complexation chemistry between the aqueous plutonium species and surface hydroxyl groups.

Plutonium−Mineral Sorption Complexes. To determine the structures of the sorbed plutonium−mineral complexes, extended XAFS (EXAFS) measurements were also made. Figure 8 shows the plutonium L_{III} edge k^3-weighted EXAFS spectra for plutonium sorbed onto manganite and hausmannite at several pH values. The data are very similar up to a k of approximately 7 $Å^{-1}$. In most cases, the best fit to the data was achieved with both a Pu−O and a Pu−Mn scattering path. Table 2 gives the best-fit parameters for the individual sorption complexes while Figures 9 and 10 show the experimental data and corresponding fits to the Fourier-filtered EXAFS and the resulting Fourier transforms for plutonium sorbed to manganite and hausmannite, respectively. The transform range for each sample was from 2.5 to 8.0 $Å^{-1}$ and was Gaussian narrowed by 0.3 $Å^{-1}$. The fit range was from 1.2 to 3.5 Å. The fits were done on each individual

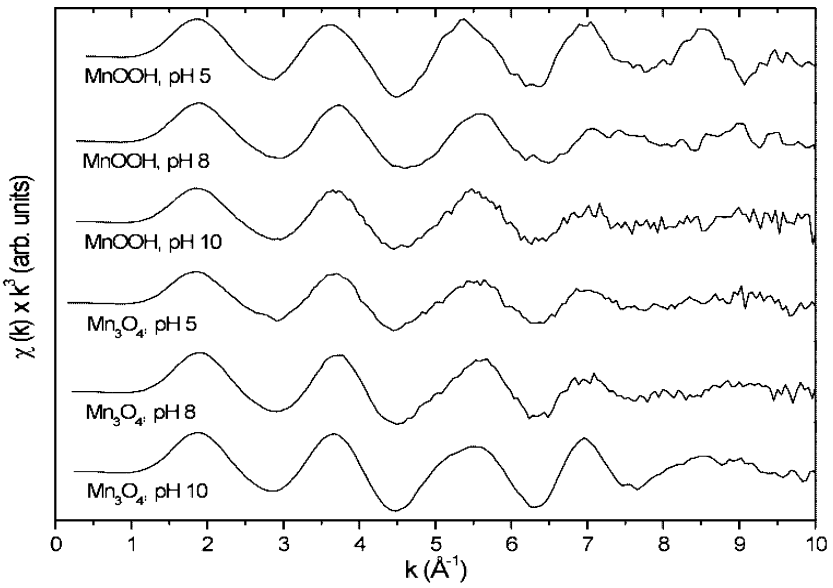

FIGURE 8. Pu L_{III} edge k^3-weighted EXAFS spectra of plutonium sorption complexes with both manganite and hausmannite at several pH values. Sample volumes and solid to solution ratios are the same as those in Figure 2. Plutonium was originally 1×10^{-4} M Pu(VI).

TABLE 2. EXAFS Structural Parameters for Plutonium Sorbed onto Manganite and Hausmannite after 24 h of Contact

mineral	pH	shell	R (Å)	N^a	σ (Å)
MnOOH	pH 5	Pu−O	2.30 ± 0.02	8.6 ± 1.3	0.12 ± 0.01
		Pu−Mn	3.37 ± 0.05	1.6 ± 1.3	0.04 ± 0.05
MnOOH	pH 8	Pu−O	2.28 ± 0.01	8.0 ± 1.3	0.12 ± 0.01
		Pu−Mn	3.42 ± 0.06	3.8 ± 2.4	0.20 ± 0.11
MnOOH	pH 10	Pu−O[b]	2.35 ± 0.01	7.0 ± 1.4	0.09 ± 0.01
Mn_3O_4	pH 5	Pu−O	2.32 ± 0.01	9.1 ± 1.6	0.13 ± 0.01
		Pu−Mn	3.37 ± 0.02	4.3 ± 3.1	0.12 ± 0.03
Mn_3O_4	pH 8	Pu−O	2.31 ± 0.01	9.3 ± 1.4	0.13 ± 0.01
		Pu−Mn	3.37 ± 0.02	4.8 ± 3.9	0.13 ± 0.04
Mn_3O_4	pH 10	Pu−O	2.36 ± 0.03	7.6 ± 1.0	0.09 ± 0.01
		Pu−Mn	3.36 ± 0.01	3.0 ± 0.6	0.09 ± 0.01

[a] The number of neighbors was calculated using $S_0^2 = 0.9 \pm 0.1$ determined from PuO_2. [b] The limited k range of these data prevented a meaningful fit to the Pu−Mn shell and is therefore excluded from these results.

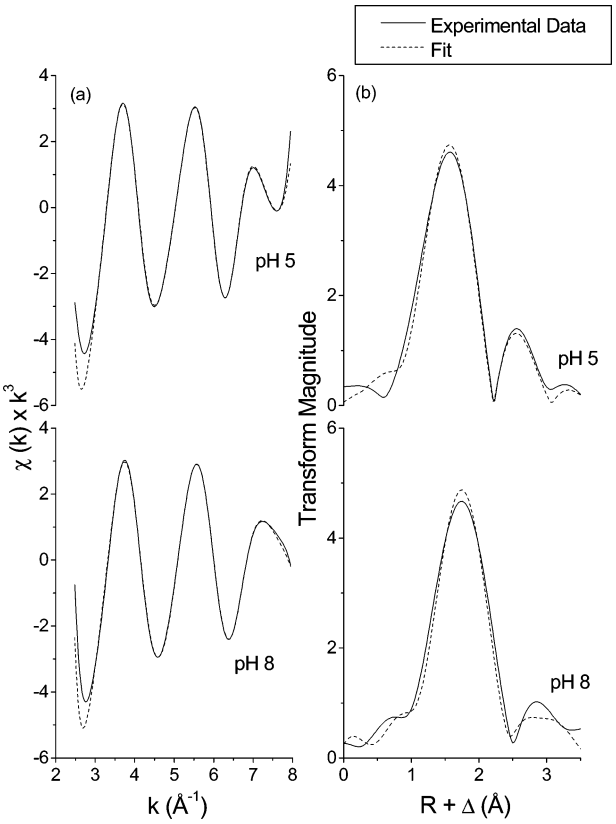

FIGURE 9. Experimental data (solid lines) and the corresponding fits (dashed lines) to the (a) Fourier-filtered EXAFS and (b) resulting Fourier transforms of plutonium sorbed to manganite (see Figure 8 for raw data). The data with manganite at pH 10 has been omitted. The transform range for each sample was 2.5−8.0 Å^{-1} and was Gaussian narrowed by 0.3 Å^{-1} during transform. The fit range was from 1.2 to 3.5 Å.

spectrum and were then averaged, thus the errors given in Table 2 are the purely statistical random errors.

Between 7.0 and 8.6 oxygen atoms are coordinated to the plutonium in the manganite samples at distances between 2.28 and 2.35 Å. The relatively large Debye−Waller factors observed for this shell indicate a broad distribution of Pu−O distances in these complexes. The distances are slightly shorter than those observed for the aquo species of Pu(IV) (*47*). This contraction of the Pu−O bond results from coordination with the mineral surface. The best fits to the second nearest neighbor shell were achieved with a Pu−Mn scattering path. Fits to this shell were also attempted with

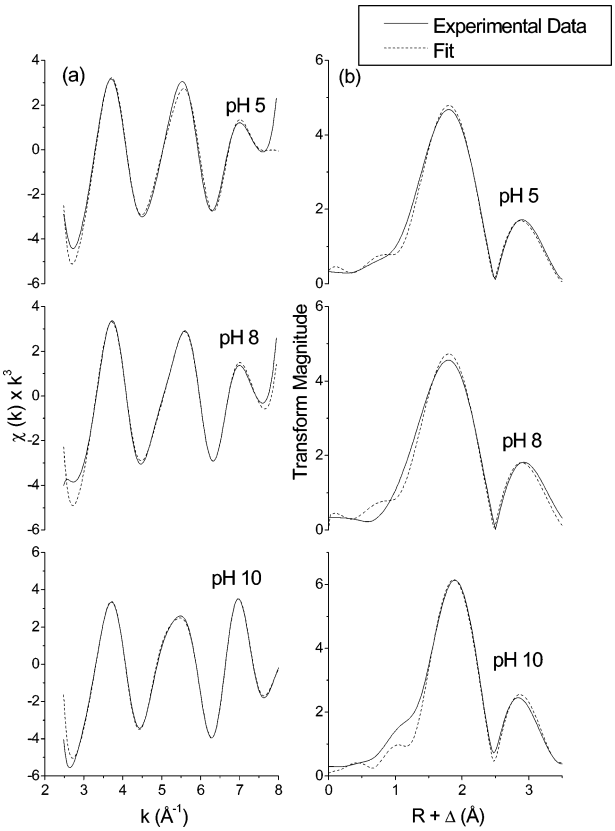

FIGURE 10. Experimental data (solid lines) and corresponding fits (dashed lines) to the (a) Fourier-filtered EXAFS and (b) resulting Fourier transforms of plutonium sorbed to hausmannite (see Figure 8 for raw data). The transform range for each sample was 2.5−8.0 Å^{-1} and was Gaussian narrowed by 0.3 Å^{-1} during transform. The fit range was from 1.2 to 3.5 Å.

carbon, oxygen, or plutonium instead of manganese, but in all cases a good quality fit to the data was not possible with any of these elements. When a carbon shell was included in the fit, the resulting bond distance was much larger than what would be expected for a solid plutonium−carbonate compound (*48*) or what is observed in similar systems such as uranium−carbonate sorption complexes (*49*). The possibility of a plutonium−carbonate compound sorbed to the mineral surfaces at high pH must be investigated further. In addition, an attempt was made to include a Pu−Pu scattering path into the fits to account for PuO_2 precipitation, but we were again unable to fit the data with this type of interaction. We therefore assume that this shell is indeed manganese even though the errors associated with the number of second nearest neighbors in Table 2 are relatively large.

The EXAFS fits lend additional support to the reduction of plutonium to Pu(IV) after contact with these minerals. If any of the oxidized, plutonyl species were present in these complexes, there would be an additional oxygen shell located around 1.8 Å from the two axial oxygens. The absence of this peak is further evidence that the plutonium is in the tetravalent state when it is sorbed to the mineral surfaces. This also supports the idea that Pu(V) observed in fits to the XANES data is due to the presence of a solution phase in these samples and not from the sorption of Pu(V) to the surfaces. The observation of an apparent Pu−Mn interaction in all samples implies that the plutonium is sorbed to the manganite and hausmannite surfaces in an inner-sphere coordination. This is similar to previously published results with iron oxyhydroxides, which have shown that actinides sorb to these minerals in an inner-sphere coordination as well (*23*, *31*, *49*, *50*). The absence of any Pu−Pu interactions

implies that the plutonium has sorbed onto the surface through complexation with the surface hydroxyl functional groups and has not simply precipitated as PuO_2. It also implies that the surface coverage is one monolayer or less because additional layers of plutonium on the surface should result in a Pu−Pu scattering peak as well.

These results indicate that manganese-based minerals could remove large quantities of plutonium from contaminated environments. Furthermore, the reduction of more oxidized plutonium species to Pu(IV) is important because Pu(IV) is much more insoluble than Pu(VI) or Pu(V) (*4*). The migration of plutonium contaminant species would be far less likely if exposure to these naturally occurring materials causes the more soluble plutonyl cations to form insoluble Pu(IV) solids. Results such as these need to be incorporated into surface complexation models to better predict the migration of plutonium contaminants through the vadose zone to groundwater supplies.

Acknowledgments

This work was supported by the Office of Science and Technology, within the U.S. Department of Energy (DOE), Environmental Management Science Program. Lawrence Berkeley National Laboratory (LBNL) and Pacific Northwest National Laboratory (PNNL) are operated by the DOE under Contracts DE-AC03-76SF00098 and DE-AC06-76RL1830, respectively. PNNL is operated by the Batelle Memorial Institute. This work was performed in part at the Stanford Synchrotron Radiation Laboratory, which is operated by the DOE, Office of Basic Energy Sciences. The authors thank the members of the Glenn T. Seaborg Center at LBNL for their assistance collecting the XAFS data.

Literature Cited

(1) Means, J. L.; Crerar, D. A.; Borcsik, M. P.; Duguid, J. O. *Geochim. Cosmochim. Acta* **1978**, *42*, 1763−1773.
(2) Sanchez, A. L.; Murray, J. W.; Sibley, T. H. *Geochim. Cosmochim. Acta* **1985**, *49*, 2297−2307.
(3) Keeney-Kennicutt, W. L.; Morse, J. W. *Geochim. Cosmochim. Acta* **1985**, *49*, 2577−2588.
(4) Cleveland, J. M. *The Chemsitry of Plutonium*; American Nuclear Society: La Grange Park, IL, 1979.
(5) Duff, M. C.; Hunter, D. B.; Triay, I. R.; Bertsch, P. M.; Reed, D. T.; Sutton, S. R.; Shea-McCarthy, G.; Kitten, J.; Eng, P.; Chipera, S. J.; Vaniman, D. T. *Environ. Sci. Technol.* **1999**, *33*, 2163−2169.
(6) Huang, P. M. In *Rates of Soil Chemical Processes*; Sparks, D. L., Suarez, D. L., Eds.; Soil Science Society of America: Madison, WI, 1991; p 191.
(7) Ehrlich, H. L. *Chem. Geol.* **1996**, *132*, 5.
(8) Waychunas, G. A. In *Reviews in Mineralogy*; Lindsley, D. H., Ed.; Mineralogical Society of America: Washington, DC, 1991; Vol. 25, p 11.
(9) Murray, J. W. *Geochim. Cosmochim. Acta* **1975**, *39*, 505.
(10) Serne, R. J.; Conca, J. L.; LeGore, V. L.; Cantrell, K. J.; Lindenmeier, C. W.; Campbell, J. A.; Amonette, J. E.; Wood, M. I. *Solid-waste leach characteristics and containment-sediment interactions. Volume 1: Batch leach and adsorption tests and sediment characterization*; Pacific Northwest National Laboratory: Richland, WA, 1993.
(11) Tebo, B. M.; Ghirose, W. C.; van Waasbergen, L. G.; Siering, P. I.; Caspi, R. In *Geomicrobiolgy Reviews in Mineralogy*; Mineralogical Society of America: Washington, DC, 1997; Vol. 35, p 225.
(12) Dachs, H. *Z. Kristallogr.* **1963**, *118*, 303.
(13) Parks, G. A.; De Bruyn, P. L. *J. Phys. Chem.* **1962**, *66*, 967−973.
(14) Cohen, D. *J. Inorg. Nucl. Chem.* **1961**, *18*, 211−218.
(15) Bucher, J. J.; Edelstein, N. M.; Osborne, K. P.; Shuh, D. K.; Madden, N.; Luke, P.; Pehl, D.; Cork, C.; Malone, D.; Allen, P. G. *Rev. Sci. Instrum.* **1996**, *67*, 1.
(16) Hayes, T. M.; Boyce, J. B. In *Solid State Physics*; Ehrenreich, H., Seitz, F., Turnbull, D., Eds.; Academic Press: New York, 1982; Vol. 37, pp 173−351.
(17) Li, G. G.; Bridges, F.; Booth, C. H. *Phys. Rev. B* **1995**, *52*, 6332−6348.
(18) Ankudinov, A. L.; Ravel, B.; Rehr, J. J.; Conradson, S. D. *Phys. Rev. B* **1998**, *58*, 1477.
(19) Dzombak, D. A.; Morel, F. M. M. *Surface Complexation Modeling*; John Wiley and Sons: New York, 1990.
(20) Davis, J. A.; Fuller, C. C.; Cook, A. D. *Geochim. Cosmochim. Acta* **1987**, *51*, 1477−1490.
(21) Fuller, C. C.; Davis, J. A. *Geochim. Cosmochim. Acta* **1987**, *51*, 1491−1502.
(22) Benjamin, M. M.; Leckie, J. O. *J. Colloid Interface Sci.* **1981**, *79*, 209−221.
(23) Waite, T. D.; Davis, J. A.; Payne, T. E.; Waychunas, G. A.; Xu, N. *Geochim. Cosmochim. Acta* **1994**, *58*, 5465−5478.
(24) Nakata, K.; Nagasaki, S.; Tanaka, S.; Sakamoto, Y.; Tanaka, T.; Ogawa, H. *Radiochim. Acta* **2000**, *88*, 453−457.
(25) Wilson, R. E.; Nitsche, H.; Shaughnessy, D. A.; Booth, C. H. Manuscript in preparation.
(26) Farr, J. D.; Schulze, R. K.; Honeyman, B. D. *Radiochim. Acta* **2000**, *88*, 675−679.
(27) Davis, J. A.; Kent, D. B. In *Mineral−Water Interface Geochemistry*; Hochella, M. F., White, A. F., Eds.; Mineralogical Society of America: Washington, DC, 1990; Vol. 23, pp 177−260.
(28) Dzombak, D. A.; Morel, F. M. M. *J. Colloid Interface Sci.* **1986**, *112*, 588−598.
(29) Kurbatov, M. H.; Wood, G. B.; Kurbatov, J. D. *J. Phys. Chem.* **1951**, *55*, 1170−1182.
(30) Rabung, T.; Geckeis, H.; Kim, J.-I.; Beck, H. P. *J. Colloid Interface Sci.* **1998**, *208*, 153−161.
(31) Kohler, M.; Honeyman, B. D.; Leckie, J. O. *Radiochim. Acta* **1999**, *85*, 33−48.
(32) Murray, J. W. *J. Colloid Interface Sci.* **1974**, *46*, 357−371.
(33) Sposito, G. *The Chemistry of Soils*; Oxford University Press: New York, 1989.
(34) Hohl, H.; Stumm, W. *J. Colloid Interface Sci.* **1976**, *55*, 281−288.
(35) Huang, C.-P.; Stumm, W. *J. Colloid Interface Sci.* **1973**, *43*, 409−420.
(36) Hsi, C.-K. D.; Langmuir, D. *Geochim. Cosmochim. Acta* **1985**, *49*, 1931−1941.
(37) Ho, C. H.; Miller, N. H. *J. Colloid Interface Sci.* **1986**, *110*, 165−171.
(38) Sagert, N. H.; Ho, C. H.; Miller, N. H. *J. Colloid Interface Sci.* **1989**, *130*, 283−287.
(39) Allen, P. G.; Bucher, J. J.; Shuh, D. K.; Edelstein, N. M.; Reich, T. *Inorg. Chem.* **1997**, *36*, 4676.
(40) Conradson, S. D.; Al Mahamid, I.; Clark, D. L.; Hess, N. J.; Hudson, E. A.; Neu, M. P.; Palmer, P. D.; Runde, W. H.; Tait, C. D. *Polyhedron* **1998**, *17*, 599.
(41) Panak, P. J.; Booth, C. H.; Caulder, D. L.; Bucher, J. J.; Shuh, D. K.; Nitsche, H. *Radiochim. Acta* **2002**, *90*, 1−7.
(42) Shaughnessy, D. A.; Nitsche, H.; Booth, C. H.; Shuh, D. K.; Waychunas, G. A.; Wilson, R. E.; Cantrell, K. J.; Serne, R. J. *J. Nucl. Sci. Technol.* **2002**, Suppl. 3, 274−277.
(43) Cohen, D. *J. Inorg. Nucl. Chem.* **1961**, *18*, 207−210.
(44) Waychunas, G. A. Personal communication.
(45) Keller, C. *The Chemistry of the Transuranium Elements*; Verlag Chemie: Weinheim, 1971.
(46) Okajima, S.; Reed, D. T. *Radiochim. Acta* **1993**, *60*, 173−184.
(47) Conradson, S. D. *Appl. Spectrosc.* **1998**, *52*, 252A−279A.
(48) Ellinger, F. H.; Zachariasen, W. H. *J. Phys. Chem.* **1954**, *58*, 405−408.
(49) Bargar, J. R.; Reitmeyer, R.; Lenhart, J. J.; Davis, J. A. *Geochim. Cosmochim. Acta* **2000**, *64*, 2737−2749.
(50) Reich, T.; Moll, H.; Arnold, T.; Denecke, M. A.; Hennig, C.; Geipel, G.; Bernhard, G.; Nitsche, H.; Allen, P. G.; Bucher, J. J.; Edelstein, N. M.; Shuh, D. K. *J. Electron. Spectrosc. Relat. Phenom.* **1998**, *96*, 237−243.

Received for review July 19, 2002. Revised manuscript received April 17, 2003. Accepted May 15, 2003.

ES025989Z